

# Use of high-resolution ultrasound as a diagnostic tool in veterinary ophthalmology

Ellison Bentley, DVM, DACVO; Paul E. Miller, DVM, DACVO; Kathryn A. Diehl, DVM, MS

**N**oninvasive visualization of the relationships between living tissues *in vivo* at a microscopic level is a goal of many imaging modalities. Recently, high-frequency ultrasound probes with frequencies ranging from 20 MHz (high-resolution ultrasound, [HRUS]) to 60 MHz (ultrasound biomicroscopy, [UBM]) have been developed that allow imaging at resolutions comparable to low-power microscopic views (20 to 80  $\mu\text{m}$ ). This represents a substantial improvement, compared with conventional 10-MHz probes that have resolutions of 300 to 400  $\mu\text{m}$ .<sup>1,2</sup> With improved image detail provided by high-frequency probes, however, tissue penetration is limited to 5 to 10 mm.<sup>3,4</sup> This depth is especially well suited to ophthalmologic applications, because the critically important structures of the anterior segment of the eye and the peripheral portions of the retina are within this range. High-resolution ultrasound fills a niche in ophthalmology in that it allows evaluation of ocular structures that cannot be fully examined by use of slit-lamp biomicroscopy or that are obscured by opacities in the aqueous humor or vitreous humor.

Reported clinical ophthalmic applications of HRUS in human ophthalmology include evaluation of tumors and cysts in the anterior segment, scleral disease, intraocular assessment of the lens, trauma, and differentiation of the various forms of glaucoma.<sup>3,5,9</sup> To our knowledge, only 1 *in vivo* study<sup>10</sup> involving UBM in dogs has been published; that report compared examination of the iridocorneal angle by use of gonioscopy and by use of UBM. Although that study revealed the potential of UBM in determining the pathogenesis of canine glaucoma, UBM often requires heavy sedation or general anesthesia in small animal patients, and patient positioning is critical in obtaining an image. Imaging with high-resolution (20 MHz) probes does not typically require anesthesia or sedation and can be performed with the animal in almost any position. The purpose of the report presented here is to describe the clinical application of HRUS in veterinary ophthalmology.

## Description of Technique

All images were obtained by use of a 20-MHz probe attached to a commercially available B-scan ultrasound machine.<sup>a</sup> The uncovered mechanical transducer was covered with a latex rubber sleeve<sup>b</sup> that had been carefully filled with distilled water to avoid entrapping air bubbles. Most animals were examined with manual restraint in sternal recumbency after topical administration of 0.5% proparacaine hydrochloride.<sup>c</sup>

One dog (case 3) required light sedation with acepromazine (0.1 mg/kg [0.045 mg/lb], IV)<sup>d</sup> and was examined in lateral recumbency. Although the probe could be easily positioned to examine the superior and temporal quadrants of the eye, light sedation was required to examine the nasal quadrant of the eye in that dog.

The eyelids were manually held open, and the probe was placed directly over the cornea or sclera. To examine the peripheral portions of the cornea and sclera, iridocorneal drainage angle, iris, ciliary body, and lens, scans were obtained with the probe held perpendicular to the globe with the scan plane perpendicular to the limbus (technique 1, longitudinal position). To examine the ciliary processes, the probe was held perpendicular to the globe with the scan plane parallel to the limbus (technique 2, transverse position). These techniques resulted in an image depth of approximately 10 mm and a resolution of 75  $\mu\text{m}$  axially and 90  $\mu\text{m}$  laterally.<sup>e</sup> When appropriate, structures were measured with the internal calipers on the ultrasound machine.

## Results

Technique 1 provided an image similar to that obtained by a traditional low-power sagittal histologic section (Fig 1 and 2). The sclera, corneal epithelium, endothelium, and Descemet's membrane were highly echogenic, whereas the corneal stroma was less echogenic, thereby allowing differentiation of the limbus. The iridocorneal angle and ciliary cleft were easily identified. The posterior epithelium of the iris was also highly echogenic. The ciliary body and processes could be easily imaged with both techniques. No complications were observed during or after performance of HRUS by use of either technique.

Five cases were selected to determine the usefulness of HRUS. A 12-year-old Quarter Horse gelding was examined because of a slowly growing red mass on the surface of the right eye of approximately 5 months' duration (case 1). Slit-lamp biomicroscopy revealed the mass to be highly vascular, cavitated, and raised; the mass arose from the temporal limbus of the right eye and extended approximately 3 mm into the conjunctiva temporally and approximately 10 mm into the cornea axially. The depth of the lesion in the cornea could not be assessed due to the opacity of the mass, but there was no apparent intraocular extension. The remainder of the ophthalmic examination findings were normal in both eyes. Differential diagnoses included hemangiosarcoma, hemangioma, angiosarcoma, other tumors, granulation tissue, abscess, foreign body reaction, squamous cell carcinoma, papilloma, habronemiasis, and onchocerciasis.<sup>11-14</sup> High-resolution ultrasound was performed, which revealed a hyperechoic mass that involved approximately one-third of

From the Department of Surgical Sciences, School of Veterinary Medicine, University of Wisconsin, Madison, WI 53706-1102.

Supported by the Steven Bechtel Foundation.

Address correspondence to Dr. Bentley.

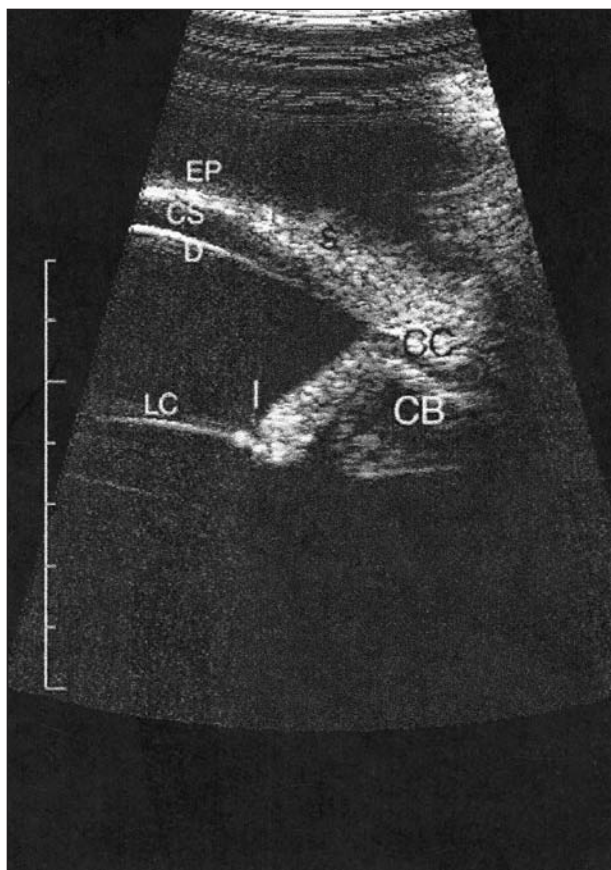


Figure 1—High-resolution ultrasound image of a healthy eye in a dog obtained with a 20-MHz probe. EP = Corneal epithelium. CS = Corneal stroma. D = Descemet's membrane. S = Sclera. LC = Anterior lens capsule. CC = Ciliary cleft. CB = Ciliary body. I = Iris. Scale indicates millimeters.

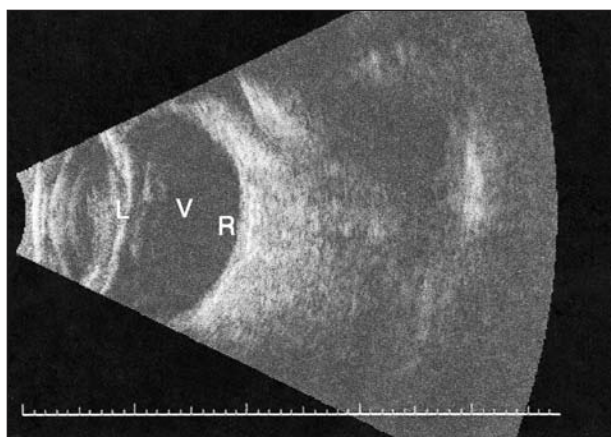


Figure 2—Ultrasound image of a normal canine eye obtained with a 10-MHz probe. L = Lens. V = Vitreous humor. R = Retina. Scale indicates millimeters.

the anterior portion of the cornea (Fig 3). On the basis of this information, excisional biopsy and cryotherapy of the surgical site were performed rather than enucleation or full-thickness corneal excision with reconstruction. The mass was identified histologically as a hemangioma. The referring veterinarian reported no recurrence 4 months postoperatively.

An 8-year-old spayed female Persian was referred

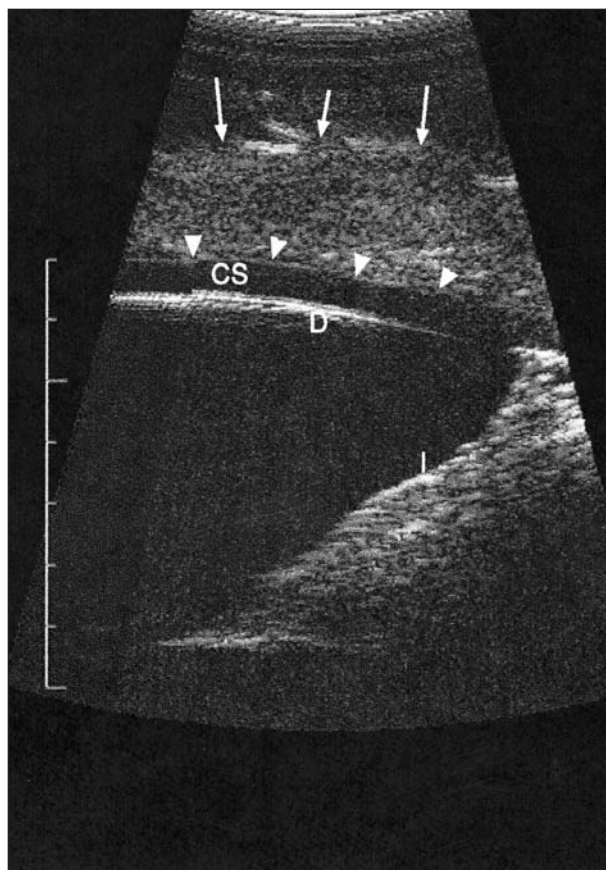


Figure 3—High-resolution ultrasound image of the right eye of a horse. Notice the mass (arrows) and normal cornea beneath the mass (arrowheads). CS = Corneal stroma. D = Descemet's membrane. I = Iris. Scale indicates millimeters.



Figure 4—Photograph of the left eye of a cat. Arrows delineate a sequestrum.

for evaluation of a corneal sequestrum of approximately 1 month's duration (case 2). Slit-lamp biomicroscopy revealed a 7-mm-diameter black, slightly raised plaque in the axial portion of the cornea of the left eye (Fig 4). The full depth of the lesion in the cornea could not be determined. Results of the remainder of the ophthalmic examination were normal in both eyes. Surgical options were discussed with the owner; however, medical treatment was initially chosen, and treatment with neomycin-polymyxin-baci-

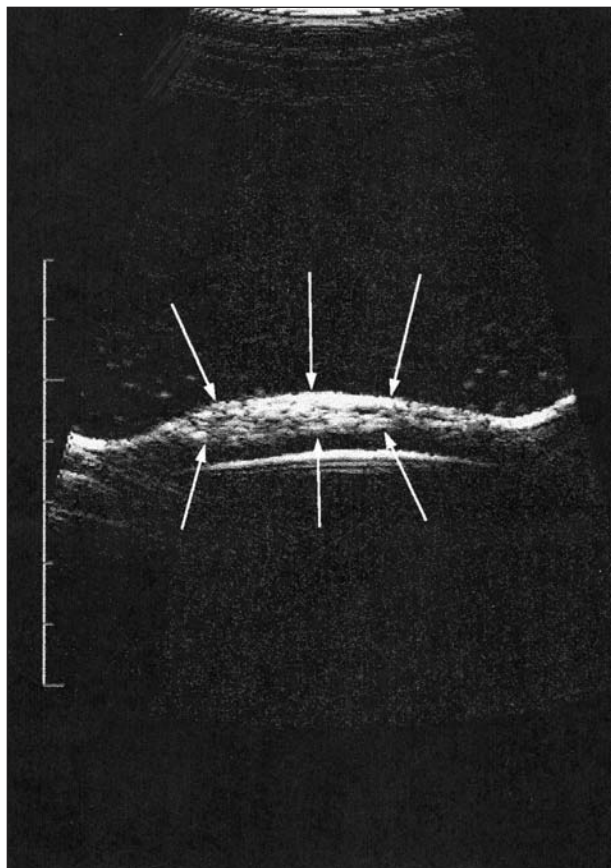


Figure 5—High-resolution ultrasound image of the cornea of the cat in Figure 4. Notice the hyperechoic, clearly demarcated lesion (arrows) extending for approximately two thirds the depth of the cornea. Scale indicates millimeters.

tracin ophthalmic ointment was instituted. The owner believed that the cat did not tolerate the medication well and therefore discontinued treatment 1 week later. Ten weeks after initial evaluation, the owner chose surgical removal of the sequestrum. Preoperative HRUS revealed that the sequestrum was hyperechoic and extended to a depth of at least two-thirds of the stromal thickness (Fig 5). The owner was advised that because of the depth of the lesion, placement of adjunctive structural support, such as that provided by lamellar keratoplasty or a conjunctival pedicle flap, would likely be necessary, and that a simple keratectomy would not suffice. A keratectomy with a lamellar keratoplasty with a frozen corneal graft was performed via a described technique.<sup>15</sup> The anterior 70% of the cornea was the most densely pigmented, and as much as 90% of the cornea was faintly pigmented. Histologic examination revealed that the anterior portion of the excised cornea was composed of degenerative collagen, whereas the deeper portion was mildly pigmented, with normal corneal stroma. The cat was routinely managed, and follow-up after surgery indicated that the cat did well without recurrence of the sequestrum.

A 2-year-old spayed female Golden Retriever was referred for evaluation of an iridal swelling in the right eye (case 3). Slit-lamp biomicroscopy revealed a mass in the peripheral nasal portion of the iris that displaced the iris anteriorly (Fig 6). A 1+ aqueous flare and 1+

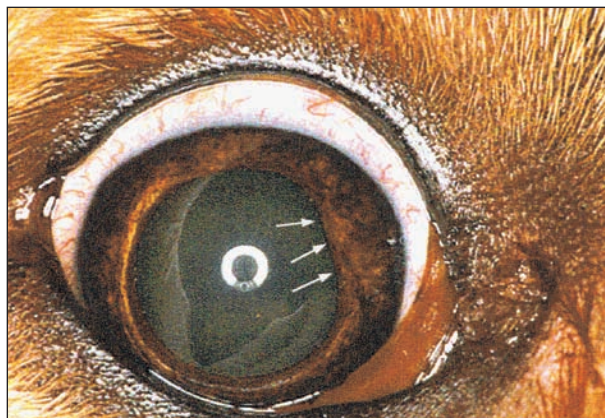


Figure 6—Photograph of the right eye of a dog with a peripheral iridal mass in the superior nasal quadrant. Arrows indicate dyscoria caused by displacement of the iris.

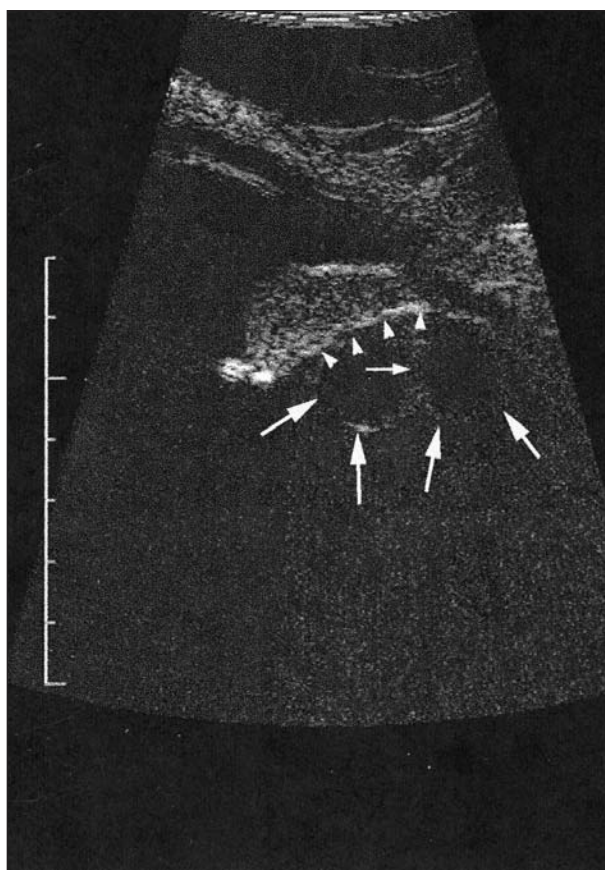


Figure 7—High-resolution ultrasound image of the eye of the dog in Figure 6. Notice the thin-walled uveal cysts (arrows) causing an iris mass effect by anterior displacement of the iris (arrowheads). Scale indicates millimeters.

anterior chamber cell count (0 = normal; 4+ = severe) was noted. An occasional pigmented cell in the anterior portion of the vitreous humor was also noted. Gonioscopy revealed that the iridocorneal drainage angle was normal, although the mass narrowed the approach to the drainage angle itself. Indirect ophthalmoscopy of the retina revealed normal findings, as did the remainder of the ophthalmic examination of both eyes. Differential diagnoses included melanocytoma of the iris, malignant melanoma of the iris, iri-

dociliary epithelial tumor, granulomas, lymphoma, and a cystic lesion of the iris or ciliary body.<sup>16-19</sup> High-resolution ultrasound revealed bilobed cysts of the peripheral portion of the ciliary body that displaced the normal portion of the iris anteriorly (Fig 7). There was no evidence of neoplasia or a cellular mass. No treatment was recommended because of the benign nature of uveal cysts.

A 6-year-old neutered male Labrador Retriever was evaluated because of swelling in the peripheral portion of the right iris (case 4). Slit-lamp biomicroscopic examination by the referring veterinary ophthalmologist revealed that the right pupil was dyscoric, and the superior portion of the right iris appeared thickened, irregular, and lighter tan in color than the surrounding tissue. There was a trace of aqueous flare and an occasional cell in the anterior chamber. Results of the remainder of the ophthalmic examination were normal. The referring ophthalmologist submitted serum for serologic examination for antibodies against *Cryptococcus* and *Toxoplasma* spp and initiated treatment consisting of administration of prednisone (0.8 mg/kg [0.36 mg/lb], PO, q 24 h) and clindamycin (8 mg/kg, [3.6 mg/lb], PO, q 12 h) and topical administration of 0.1% dexamethasone ophthalmic suspension every 8 hours in the right eye for 2 weeks. Two weeks later, the appearance of the iris was unchanged, serologic results were negative, and the dog was referred for evaluation with HRUS. Results of ophthalmic examination were similar to previous examinations and peripheral anterior synechia in the region of the thickened iris was also seen via gonioscopic examination. High-resolution ultrasound revealed the iris to be diffusely thickened with a homogeneous echogenicity and indistinct borders (Fig 8). The ciliary cleft was open. Differential diagnoses included melanocytoma of the iris, malignant melanoma of the iris, iridociliary epithelial tumor, lymphoma, or granuloma. Diagnostic and therapeutic options offered to the owner included needle aspiration, incisional biopsy, and enucleation. Risks associated with needle aspiration and biopsy included the low diagnostic yield of cytologic examination for intraocular tumors, intraocular hemorrhage, and retinal detachment.<sup>20</sup> The owners chose removal of the eye because of their concerns about the possibility of a potentially aggressive neoplastic process. Histopathologic findings included localized lymphogranulomatous iritis. The superior portion of the iris was thickened by a cellular infiltrate of lymphoplasmacytic inflammatory cells and smaller cells containing melanin. The etiology of the granuloma was unknown.

A 9-year-old spayed female mixed-breed dog was examined because of vision loss (case 5). The medical history included a diagnosis of diabetes mellitus 4 months previously; this disease was well controlled by parental administration of insulin. Initial ophthalmic examination revealed that direct and consensual pupillary light reflexes were present but sluggish, and menace responses were absent in both eyes. The left eye was mildly buphthalmic. Slit-lamp biomicroscopy revealed shallow anterior chambers in both eyes, 1+

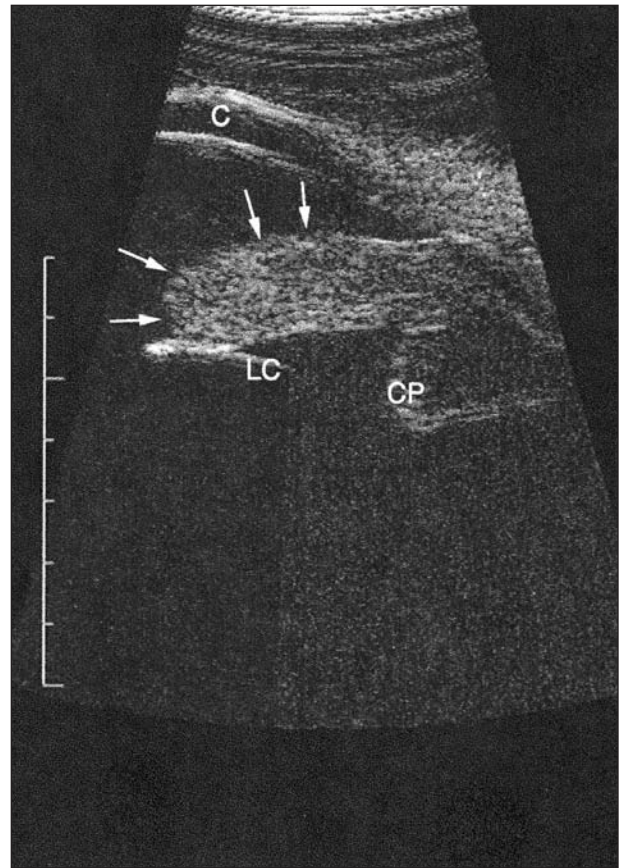


Figure 8—High-resolution ultrasound image of the right eye of dog evaluated for a peripheral iridal swelling. Notice the thickened iris (arrows) with homogeneous echogenicity consistent with a mass. LC = Lens capsule. C = Cornea. CP = Ciliary process.

anterior chamber flare in the right eye, 2+ anterior chamber flare in the left eye, mild corneal edema with keratic precipitates in both eyes, and complete cataracts in both lenses. Posterior synechiae and rubeosis iridis were detected in the left eye. Intraocular pressures measured by use of applanation tonometry were 12 mm Hg in the right eye and 16 mm Hg in the left eye. B-scan ultrasonography with a 10-MHz probe revealed multiple, free floating, hyperechoic vitreal opacities and hyperechogenicity of the lens in both eyes. High-resolution ultrasound (but not the traditional 10-MHz ultrasound) revealed a peripheral equatorial lens capsule disruption with extrusion of lens material in the left eye (Fig 9). The ciliary cleft also appeared collapsed, which was consistent with previous glaucoma and buphthalmia. The ruptured lens capsule was judged to be the cause of the difference in the inflammatory changes between the 2 eyes. Surgical options were discussed with the owners, and they were informed that the left eye was at increased risk for chronic inflammation and continuing glaucoma because of the ruptured lens capsule. Lensectomy would have the best chance at avoiding phacoclastic uveitis secondary to lens rupture;<sup>4</sup> however, preexisting uveitis has been associated with an increased risk of postoperative complications.<sup>21</sup> The owners chose not to pursue surgery; therefore, anti-inflammatory treatment was instituted.

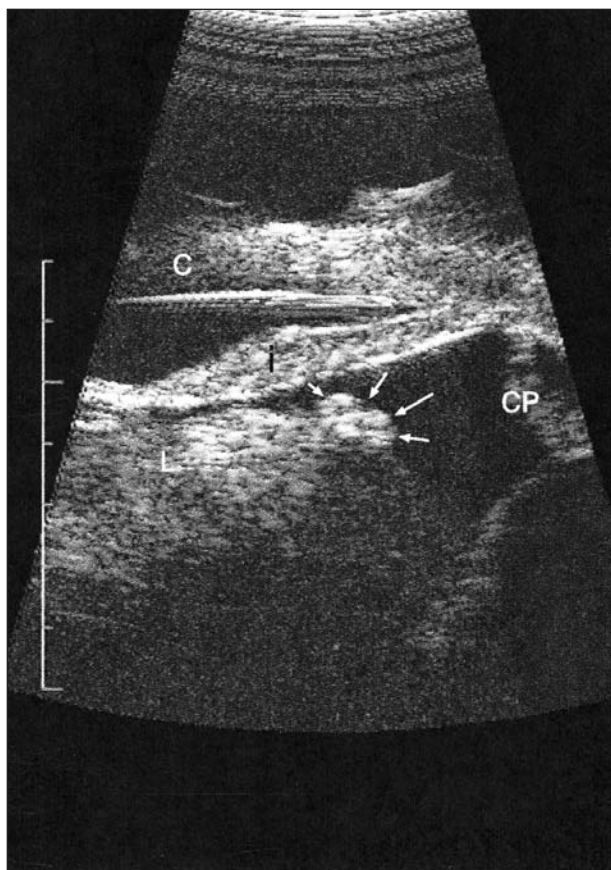


Figure 9—High-resolution ultrasound image of the left eye of a dog with diabetic cataracts and associated uveitis. Notice the area of lens capsule disruption (arrows). C = Cornea. i = Iris. L = Lens. CP = Ciliary process.

## Discussion

High-resolution ultrasound with a 20-MHz transducer was a useful diagnostic tool in this case series. High-resolution ultrasound expanded the capability of the clinician to distinguish among various anterior segment diseases and more effectively develop therapeutic strategies. In contrast to UBM, which is performed via general anesthesia and with a 50- to 60-MHz probe, HRUS was easily performed in awake or lightly sedated animals with only topical anesthesia. Although image resolution with HRUS is not as good as that with UBM, the ability to perform HRUS in awake patients offered a number of distinct advantages over UBM in a clinical setting including reduced complications from the procedure, reduced expense, ability to perform sequential examinations minutes to hours apart, and freedom from artifactual changes in pupil size and accommodation associated with general anesthesia. Additionally, image quality with HRUS was adequate to discern the relevant anatomic structures. No adverse effects attributable to HRUS were detected, suggesting it is a safe procedure in a clinical setting.

The 20-MHz HRUS was a valuable adjunct to slit-lamp biomicroscopy in the evaluation of corneal opacification secondary to corneal sequestrum and neoplasia of the ocular surface. Typically, opacification involving the anterior portion of the cornea obscures or completely prevents direct determination of the full extent

and depth to which the lesion involves the cornea. This complicates surgical planning, and often the surgeon is required to intraoperatively determine whether a simple keratectomy, full-thickness eyewall resection with a reconstructive procedure, or even enucleation is necessary. Faintly pigmented or early sequestrum lesions may not be accurately imaged because they do not cause enough alteration of the corneal stroma to alter the passage of sound waves. The deeper, faintly pigmented portion of the sequestrum was not apparent on the HRUS image in case 2, which correlated with the histologic appearance of degenerative collagen anteriorly, but HRUS allowed a better assessment than slit-lamp biomicroscopy. It also permitted the surgeon to determine that the tumor of the ocular surface in case 1 did not invade into the globe, and that surface treatment would likely be adequate. Estimates of the depth of corneal involvement may not be precisely accurate due to variations in the speed of sound in diseased corneal tissue versus that in normal cornea.

Iridal or ciliary body tumors and cysts are common ocular abnormalities in domestic animals.<sup>17</sup> Differentiating between these entities, as well as other causes of iris displacement such as iris bombé and lens intumescence, is critical in maximizing the visual outcome and comfort of the patient. Anterior uveal tumors, although generally benign in dogs,<sup>16,17</sup> can result in substantial ocular damage and loss of vision and are therefore usually treated by use of laser photocoagulation, iridectomy, iridocyclectomy, or enucleation.<sup>17,19,22</sup> Uveal cysts, however, pose little threat to ocular health and are usually simply observed. Iris bombé can mimic extensive retroiridal cyst formation as well as ciliary body tumor. Additionally, anterior chamber shallowing because of swelling and anterior displacement of the lens can also appear clinically similar to iris bombé. The HRUS permitted these entities to be readily differentiated from each other in this case series, although at this time HRUS cannot differentiate tumors from granulomas. The HRUS also allowed explanation of the different degrees of uveitis between eyes in the dog with rupture of the lens capsule and allowed the clinician to better plan possible cataract surgery.

On the basis of the image quality of the irido-corneal angles in this case series, HRUS would also appear to be useful in elucidating the mechanisms by which the various forms of glaucoma may develop. It may also be a useful tool in investigating the mechanism by which various anti-glaucoma drugs lower intraocular pressure in domestic animals. Such critical measurements as the length, width, and area of the ciliary cleft, as well as the degree of iris-lens contact and angle opening distance, can be reliably measured with HRUS.<sup>8</sup> Other potential uses include more critical evaluation of cats with slowly progressive diffuse melanoma of the iris. It has been reported that cats with diffuse iridal involvement have similar survival times as control groups, but that those tumors that involve other structures, such as the ciliary body, or have aggressive infiltration of the iris and its posterior epithelium are associated with increased mortality rates.<sup>23</sup> Prior to the development of HRUS and UBM,

however, the clinician had no reliable method of determining whether these events had occurred. The HRUS may allow these cats to be more effectively monitored and maximize the time the eye is retained without increasing the risk of metastasis. Finally, HRUS may be a useful teaching aid, because the image allows the student to see the depth of a corneal ulcer or other anterior segment lesions that are difficult to view with other examination techniques.

<sup>a</sup>T<sup>3</sup> B-scan, Innovative Imaging Inc, Sacramento, Calif.

<sup>b</sup>Vision Care Devices Inc, Redding, Calif.

<sup>c</sup>Bausch & Lomb Pharmaceuticals, Tampa, Fla.

<sup>d</sup>Fort Dodge Animal Health, Fort Dodge, Iowa.

<sup>e</sup>Kendall C, Innovative Imaging Inc, Sacramento, Calif: Personal communication, 2002.

<sup>f</sup>Wilkie DA, Gemensky A, Morreale RJ, et al. Spontaneous lens capsule rupture secondary to diabetes mellitus: surgical outcome in canine eyes (abstr), in *Proceedings. Am Coll Vet Ophthalmol* 2002;45.

<sup>g</sup>Bentley E, Diehl KA, Miller PE. Measurement of high resolution ultrasound images: intraobserver and interobserver reliability (abstr), in *Proceedings. Am Coll Vet Ophthalmol* 2002;64.

## References

1. Reminick L, Finger P, Ritch R, et al. Ultrasound biomicroscopy in the diagnosis and management of anterior segment tumors. *J Am Optom Assoc* 1998;69:575–581.
2. Verbeek A. Conventional diagnostic ultrasound of the iris lesions. *Doc Ophthalmol* 1995;90:43–52.
3. Foster F, Pavlin C. Advances in ultrasound biomicroscopy. *Ultrasound Med Biol* 2000;26:1–27.
4. Pavlin C, Foster F. Ultrasound biomicroscopy: high-frequency ultrasound imaging of the eye at microscopic resolution. *Radiol Clin North Am* 1998;36:1047–1058.
5. Deschenes J, Mansour M, Rudzinski M. Ultrasound and ultrasound biomicroscopy as a diagnostic tool. *Dev Ophthalmol* 1999;31:14–21.
6. Marigo F, Esaki K, Finger P, et al. Differential diagnosis of anterior segment cysts by ultrasound biomicroscopy. *Ophthalmology* 1999;106:2131–2135.
7. Ritch R, Liebmann J. Role of ultrasound biomicroscopy in the differentiation of block glaucomas. *Curr Opin Ophthalmol* 1998;9:39–45.
8. Kobayashi H, Hirose M, Kobayashi K. Ultrasound biomicroscopic analysis of pseudophakic pupillary block glaucoma induced by Soemmering's ring. *Br J Ophthalmol* 2000;84:1142–1146.
9. Marigo F, Finger P, McCormick S, et al. Iris and ciliary body melanomas: ultrasound biomicroscopy with histopathologic correlation. *Arch Ophthalmol* 2000;118:1515–1521.
10. Gibson TE, Roberts SM, Severin GA, et al. Comparison of gonioscopy and ultrasound biomicroscopy for evaluating the irido-corneal angle in dogs. *J Am Vet Med Assoc* 1998;213:635–638.
11. Brooks D. Equine ophthalmology. In: Gelatt K, ed. *Veterinary ophthalmology*. 3rd ed. Philadelphia: Lippincott Williams & Wilkins, 1999;1053–1116.
12. Bolton J, Lees M, Robinson W, et al. Ocular neoplasms of vascular origin in the horse. *Equine Vet J* 1990;suppl 10:73–75.
13. Hacker DV, Moore PF, Buyukmihci NC. Ocular angiosarcoma in four horses. *J Am Vet Med Assoc* 1986;189:200–203.
14. Moore PF, Hacker DV, Buyukmihci NC. Ocular angiosarcoma in the horse: morphological and immunohistochemical studies. *Vet Pathol* 1986;23:240–244.
15. Gimenez M, Farina I. Lamellar keratoplasty for the treatment of corneal sequestrum. *Vet Ophthalmol* 1998;1:163–166.
16. Dubielzig R. Ocular neoplasia in small animals. *Vet Clin North Am Small Anim Pract* 1990;20:837–848.
17. Collins B, Moore C. Diseases and surgery of the canine anterior uvea. In: Gelatt K, ed. *Veterinary ophthalmology*. 3rd ed. Philadelphia: Lippincott Williams & Wilkins, 1999;755–795.
18. Wilcock B, Peiffer R. Morphology and behavior of primary ocular melanomas in 91 dogs. *Vet Pathol* 1986;23:418–424.
19. Peiffer R, Wilcock B, Dubielzig R, et al. Fundamentals of veterinary ophthalmic pathology. In: Gelatt K, ed. *Veterinary ophthalmology*. 3rd ed. Philadelphia: Lippincott Williams & Wilkins, 1999;355–426.
20. Cook C, Davidson M, Brinkmann M, et al. Diode laser transscleral cyclophotocoagulation for the treatment of glaucoma in dogs: results of six and twelve month follow-up. *Vet Comp Ophthalmol* 1997;7:148–154.
21. Paulsen M, Lavach J, Severin G, et al. The effect of lens-induced uveitis on the success of extracapsular cataract extraction: a retrospective study of 65 lens removals in the dog. *J Am Anim Hosp Assoc* 1986;22:49–56.
22. Cook C, Wilkie D. Treatment of presumed iris melanoma in dogs by diode laser photocoagulation: 23 cases. *Vet Ophthalmol* 1999;2:217–225.
23. Kalishman J, Dubielzig R, Chappell R, et al. A matched observational study of survival in cats with enucleation due to diffuse iris melanoma. *Vet Ophthalmol* 1998;1:25–29.